Evaluation of In-room Volumetric Imaging Doses for Image-guided Radiotherapy: A Multi-institutional Study

Yusuke Sakai[1,2], Hajime Monzen[1], Yoshiki Takei[3], Hiroyuki Kosaka[1], Kenji Nakamura[1], Yuya Yanagi[1], Kazuki Wakabayashi[1], Makoto Hosono[4], Yasumasa Nishimura[4]

[1]Department of Medical Physics, Graduate School of Medical Sciences, Kindai University, [2]Department of Radiotherapy, Takarazuka City Hospital, Takarazuka, Hyogo, [3]Department of Radiology, Kindai University Nara Hospital, Ikoma, Nara, [4]Department of Radiation Oncology, Faculty of Medicine, Kindai University, Osakasayama, Osaka, Japan

Abstract

Aims: We investigated imaging dose and noise under clinical scan conditions at multiple institutions using a simple and unified method, and demonstrated the need for diagnostic reference levels in image-guided radiotherapy (IGRT). **Materials and Methods:** Nine cone-beam and helical computed tomography (CT) scanners (Varian, Elekta, Accuray Inc., and BrainLAB) from seven institutions were investigated in this study. The weighted cone-beam dose index ($CBDI_w$) was calculated for head and pelvic protocols using a 100 mm pencil chamber under the conditions used in actual clinical practice at each institution. Cone-beam CT image noise was evaluated using polymethylmethacrylate head and body phantoms with diameters of 16 and 32 cm, respectively. **Results:** For head and pelvic protocols, $CBDI_w$ values ranged from 0.94–6.59 and 1.47–20.9 mGy, respectively. Similarly, standard deviation (SD) values ranged from 9.3–34.0 and 26.9–97.4 HU, respectively. The SD values tended to increase with decreasing imaging dose ($r = -0.33$ and -0.61 for the head and pelvic protocols, respectively). **Conclusions:** Among the nine machines, the imaging dose for high imaging dose institutions was approximately 20 mGy to the pelvic phantom, and there was a 14-fold difference in dose compared with the other institutions. These results suggest the need to establish DRLs for IGRT to guide clinical decision-making.

Keywords: Diagnostic reference level, image-guided radiotherapy, imaging dose

INTRODUCTION

Medical radiation exposure is increasing with advancements in radiology and now accounts for about 20% of all radiation exposure worldwide; this figure is even higher in developed countries.[1,2] The International Commission on Radiological Protection supports the "as low as reasonably achievable" (ALARA) principle,[3] which intends to reduce unnecessary exposure. Optimization of imaging doses is important for incorporating the ALARA principle. In the field of diagnostic radiology, diagnostic reference levels (DRLs) are commonly used as the reference levels for different imaging modalities.[4] The DRL is defined as the 75th percentile of the imaging dose distribution and helps institutions determine whether their dose levels accord with those of other centers.[4]

Image-guided radiotherapy (IGRT) is becoming increasingly important given the greater use of high-precision radiotherapy.[5-8] One problem with IGRT is that normal tissues outside the treatment field are exposed to radiation because the imaging field is larger than the treatment field.[9] In recent years, IGRT has generally been performed before every treatment, which increases the imaging dose and affects the optimized planning dose to the treatment area.[10,11] Therefore, the radiotherapy imaging dose should be optimized in accordance with the ALARA principle. However, no reference IGRT imaging dose has been established, and dose variations are unclear because imaging conditions are at the discretion of each individual institution.

Address for correspondence: Mr. Yusuke Sakai, Department of Medical Physics, Graduate School of Medical Sciences, Kindai University, 377-2 Onohigashi, Osakasayama, Osaka 589-8511, Japan. E-mail: ysakai.kmsyo@gmail.com

Access this article online

Quick Response Code:

Website: www.jmp.org.in

DOI: 10.4103/jmp.jmp_109_22

Many previous studies have reported imaging doses for default protocols, but few have investigated them in the context of the actual protocols used in clinical practice.[12-15] In addition, the imaging dose also depends on the measurement tool and points, phantom size, and imaging techniques. Hence, unified measurement method and evaluation index are crucial for multi-institution surveys. In this study, we used polymethylmethacrylate (PMMA) phantoms and a 100 mm pencil chamber, which are widely employed tools, to evaluate imaging dose and image quality.

This study focused on in-room cone-beam computed tomography (CBCT) and helical CT imaging. We investigated the imaging dose and image quality of head and pelvic protocols under clinical scan conditions for nine treatment machines at seven institutions using a simple and unified method for CT imaging before every treatment. Then, we demonstrated the need for DRLs in IGRT for the purpose of optimization and standardization of IGRT imaging doses.

MATERIALS AND METHODS

Dose measurements were performed using the 32 cm diameter PMMA body phantom, 16 cm diameter head phantom (15 cm in length), and 100 mm pencil chamber of each participating institution. The scanning protocols were set according to the conditions used in clinical practice at each institution for head and pelvic regions (except those for stereotactic radiotherapy). Tables 1 and 2 list the clinical scan conditions and provide examples of preset mAs values for head and pelvic protocols for the nine IGRT-CT machines. Institution C does not utilize filters as the device settings have remained unchanged since installation. In lieu of filters, they minimize the mAs value as much as possible to reduce radiation exposure. Institution G uses a small field of view (FOV) for their pelvic protocol, but to align the conditions for noise evaluation with those of other institutions, a 32 cm body phantom is also used. For ClearRT imaging using the Radixact® helical tomotherapy system (Accuray, Sunnyvale, CA, USA) in institution E, the "medium" body size and "normal" scanning mode presets are used; scanning parameters are detailed in a previous study.[16]

The cone-beam dose index (CBDI) was used to evaluate the imaging dose for the head and pelvic protocols using head and body phantoms, respectively.[13,17-19] The pencil chamber was inserted into the central and peripheral (0°, 90°, 180°, and 270°) parts of the phantom. Measurements were obtained three times in each position and averaged, and the CBDI was then calculated as follows:

$$CBDI = \frac{1}{100} D_{100\,mm} \qquad (1)$$

where $D_{100\,mm}$ represents the dose absorbed across the 100 mm chamber, and 100 is the sensitive length of the chamber. Then, weighted CBDI ($CBDI_w$) was calculated as follows:

$$CBDI_w = \frac{1}{3} CBDI_{center} + \frac{2}{3} CBDI_{peripheral} \qquad (2)$$

where $CBDI_{center}$ is the CBDI at the center of the phantom and $CBDI_{peripheral}$ is the average CBDI of the four peripheral positions. We also calculated nCBDIw, which is the normalized CBDIw value per 100 mAs of gantry rotation in the clockwise direction; the same direction was used for all machines to reduce the influence of rotation direction on the measured value.[20] The CBDI and CT dose index (CTDI) are generally measured when the couch is static; however, for the ClearRT helical fan beam CT system, the couch is moving during gantry rotation. Hence, for the ClearRT system, helical measurements were performed with a scan range equal to the phantom length divided by 100 mm, which corresponds to the "volume CBDI" ($CBDI_{vol}$).[21] Then, $CBDI_w$ was calculated by dividing $CBDI_{vol}$ by the pitch factor. We also investigated the methods employed in each institution for reducing the imaging dose.

The PMMA phantom is made of homogeneous acrylic material and can be used as a phantom for noise measurement, as described in the American Association of Physicists in Medicine Task Group (AAPM TG) Report 233.[22] In addition, particularly in the pelvic region, the Catphan phantom is smaller than the patient's body, and larger phantoms are useful for noise measurement and have been used in several papers.[23,24] Therefore, we evaluated noise in CBCT or helical CT images using the PMMA phantom acquired during dosimetry. Image noise was quantified according to the standard deviation (SD) of pixel values in the region of interest (ROI). As well as allowing for dose measurement, the PMMA phantom can be also used for noise evaluation because of its uniformity, as described in AAPM TG Report 233.[22] The ROI size was set to 1% of the diameter of the phantom area in the images (for the 10 central slices). Five ROIs were placed (one in the center and four in peripheral locations located at a distance from the phantom edge in the FOV equal to the ROI diameter), avoiding "plug holes" [Figure 1]. To evaluate image noise, SD values were calculated for each ROI. To examine differences in SD values in individual ROIs, we also calculated the SD of "SD values" among ROIs (i.e., the SD of SD), and divided it by the mean SD value, which was the coefficient of variation (CV) of the "SD value." CV_{total} represents the CV calculated from five ROIs and CV_{peri} represents the CV calculated from the only four peripheral ROIs.

RESULTS

Figure 2 shows the example CBCT images of head and body PMMA phantoms acquired at institution D. Artifacts appear near the center of the body phantom, which was also observed in images from other institutions. Tables 3 and 4 show the imaging dose and image noise data for the head and pelvic protocols. $CBDI_w$ ranged from 0.94–6.59 mGy for the head protocol and 1.47–20.9 mGy for the pelvic protocol among the nine machines. The maximum difference in imaging dose was 7-fold between institutions E and F for the head protocol and 14-fold
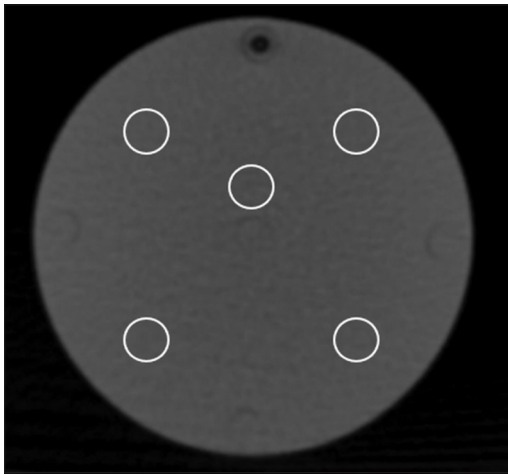
Figure 1: Regions of interest (ROIs) for the noise measurements. ROIs were generated at the center and four peripheral locations, avoiding the "plug hole." The ROIs in peripheral locations were located at a distance from the phantom edge in the FOV equal to the ROI diameter. ROIs: Regions of interest, FOV: Field of view

between institutions C and D for the pelvic protocol. Some institutions employed methods for reducing the pelvic imaging dose. In institution C, which had the lowest dose (1.47 mGy), bone or high-contrast object matching is performed in the pelvic region, and gold markers or seeds are inserted in all cases of prostate cancer. Institutions G and F, which had the second and third lowest doses (4.17 and 5.70 mGy, respectively), use a full fan mode with a gantry rotation angle of 200°, similar to a head protocol with a lower mAs value. Institution A, which uses the Halcyon scanner (Varian Medical Systems, Palo Alto, CA, USA) and had the fourth lowest dose (6.61 mGy), applies the reduced mAs value determined on the basis of an offline phantom evaluation considering visibility and dose. The four machines with the highest imaging doses (at institutions B, D, and E) use the default mAs value.

The average CV_{total} was 0.07 for the head protocol and 0.22 for the pelvic protocol. The CV_{total} value for the body phantom was higher than that for the head phantom, because the SD for the center ROI was high because of an artifact

Table 1: Head scan conditions

	Institution								
	A		**B**		**C**	**D**	**E**	**F**	**G**
Treatment machine	TrueBeam XI	Halcyon kVI	TrueBeam XI	Novalis Tx OBI	Synergy XVI	Clinac iX OBI	Tomotherapy ClearRT	Synergy XVI	TrueBeam XI
Tube voltage (kV)	100	100	100	100	110	100	100	100	100
Total mAs	150	126	150	145	46.8	72	300	39.2	150
Superior-inferior collimation (cm)	18.5	13.2	18.5	16	27.7	16	10	27.7	18.5
Gantry rotation range (°)	200	360	202	202	200	204	-	200	200
Filtration	Full bowtie	Full bowtie	Full bowtie	Full bowtie	-	Full bowtie	0.5 mm	Full bowtie	Full bowtie
FOV (mm)	500	492	464.9	450	270	450	440	270	262
Slice thickness (mm)	2	2	2	2.5	1	1	2	1	2
Preset mAs	150	126	150	145	46.8	145	470	36.6	150

FOV: Field of view, OBI: On-board imager

Table 2: Pelvic scan conditions

	Institution								
	A		**B**		**C**	**D**	**E**	**F**	**G**
Treatment machine	TrueBeam XI	Halcyon kVI	TrueBeam XI	Novalis Tx OBI	Synergy XVI	Clinac iX OBI	Tomotherapy ClearRT	Synergy XVI	TrueBeam XI
Tube voltage (kV)	125	125	125	125	110	125	140	120	125
Total mAs	540	280	1080	680	46.8	680	896	250.9	200
Superior-inferior collimation (cm)	18.5	13.2	17.5	16	27.7	16	10	27.7	18.5
Gantry rotation range (°)	360	360	360	364	200	364	-	200	200
Filtration	Half bowtie	Half bowtie	Half bowtie	Half bowtie	-	Half bowtie	Al bowtie	Half bowtie	Full bowtie
FOV (mm)	500	492	464.9	450	270	450	440	270	262
Slice thickness (mm)	2	2	2	2.5	1	1	2	1	2
Matching object	Soft-tissue	Soft-tissue	Soft-tissue	Soft-tissue	Bone/marker	Soft-tissue	Soft-tissue	Soft-tissue	Soft-tissue
Preset mAs	1080	560	1080	680	585.6	680	896	1056	1080

FOV: Field of view, OBI: On-board imager

**Table 3: Summary of the imaging dose and noise for the head protocols**

	Institution								
	A		**B**		**C**	**D**	**E**	**F**	**G**
Treatment machine	**TrueBeam XI**	**Halcyon kVI**	**TrueBeam XI**	**Novalis Tx OBI**	**Synergy XVI**	**Clinac iX OBI**	**Tomotherapy ClearRT**	**Synergy XVI**	**TrueBeam XI**
CBDI$_w$ (mGy)	3.86	3.91	4.00	4.05	2.26	2.53	6.59	0.94	3.81
nCBDI$_w$ (mGy/100 mAs)	2.57	3.10	2.67	2.72	4.83	3.52	1.83	2.41	2.54
SD$_{peri}$ (HU)	25.9	-	23.4	26.9	12.0	34.0	9.3	20.7	21.5
CV$_{total}$	0.06	-	0.06	0.08	0.12	0.06	0.07	0.09	0.06
CV$_{peri}$	0.03	-	0.04	0.08	0.13	0.05	0.06	0.09	0.04

CBDI$_w$: Weighted cone-beam dose index, nCBDI$_w$: Normalized CBDI$_w$, SD: Standard deviation, CV: Coefficient of variation, OBI: On-board imager

Table 4: Summary of the imaging dose and noise for the pelvic protocols

	Institution								
	A		**B**		**C**	**D**	**E**	**F**	**G**
Treatment machine	**TrueBeam XI**	**Halcyon kVI**	**TrueBeam XI**	**Novalis Tx OBI**	**Synergy XVI**	**Clinac iX OBI**	**Tomotherapy ClearRT**	**Synergy XVI**	**TrueBeam XI**
CBDI$_w$ (mGy)	9.41	6.61	18.82	19.95	1.47	20.9	11.3	5.70	4.17
nCBDI$_w$ (mGy/100 mAs)	1.74	2.36	1.74	2.87	3.14	3.07	1.57	2.27	2.09
SD$_{peri}$ (HU)	59.6	-	27.5	35.5	83.2	49.0	26.9	31.3	97.4
CV$_{total}$	0.39	-	0.59	0.28	0.12	0.02	0.13	0.12	0.07
CV$_{peri}$	0.12	-	0.07	0.03	0.07	0.02	0.14	0.07	0.06

CBDI$_w$: Weighted cone-beam dose index, nCBDI$_w$: Normalized CBDI$_w$, SD: Standard deviation, CV: Coefficient of variation, OBI: On-board imager
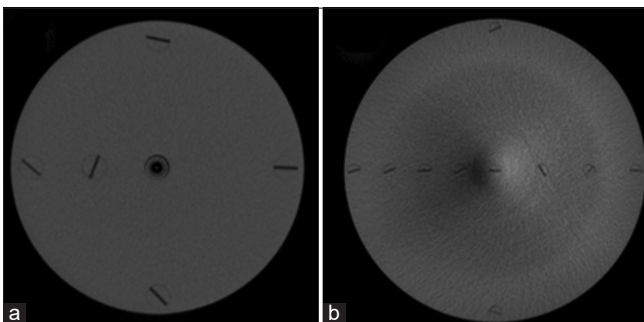
Figure 2: Cone-beam CT images of the PMMA phantom: (a) head; (b) body. CT: Computed tomography, PMMA: Polymethylmethacrylate

around the center of the body phantom. The average CV$_{peri}$ value was 0.06 for the head protocol and 0.07 for the pelvic protocol. The use of ROIs only in peripheral positions reduces the variability of SD among ROIs. Hence, SD$_{peri}$, which is the SD value calculated from ROIs in peripheral positions only, was applied as a noise indicator. The SD value for the Halcyon scanner was excluded because an iterative image reconstruction algorithm was used and the data did not follow a normal distribution. SD$_{peri}$ ranged from 9.3–34.0 HU for the head protocol and 26.9–97.4 HU for the pelvic protocol; in both cases, there was an approximately 3.6-fold difference between the machines with the highest and lowest values. Figure 3 shows the CBDI$_w$ (denoted by "•") and SD$_{peri}$ (denoted by "△") values for each machine, plotted in order of magnitude (low to high). SD$_{peri}$ tended to decrease with increasing CBDI$_w$, and the correlation coefficients (*r*)

were −0.33 and −0.61 for the head and pelvic protocols, respectively.

DISCUSSION

Using a simple and unified method, we investigated imaging dose and image noise under the conditions used in clinical practice at seven institutions for nine treatment machines. For a multi-institutional survey, measurement methods and evaluation indices, which are easy to implement in any institution, will be needed. The CTDI, which is the most popular index, is not ideal for wide beam modalities such as CBCT because of dose underestimation caused by an insufficient detector and phantom length.[25-29] The methodology described in International Atomic Energy Agency Human Health Report No. 5. requires multiple or longer chambers for wide beam widths and measurement of CTDI in both the air and phantom. In addition, the methodology described in AAPM TG Report 111 requires numerous additional scatterers, as well as a beam quality correction factor for kilovoltage X-ray, making these methods complicated.[25,26] The CBDI provides a measure of the dose comparable to that of the method in AAPM TG Report 111 but has the advantages of a simple measurement method and easy implementation in many institutions because of its use of commonly available tools.[27] In the previous study, the CTDIw values of the Varian TrueBeam for head and pelvic protocols were 2.3 and 1.7 mGy/mAs, respectively. In this study, the average CBDIw values of the three Varian TrueBeam machines were higher at 2.6 and 1.9 mGy/mAs, respectively.[28] For image quality evaluation, highly uniform
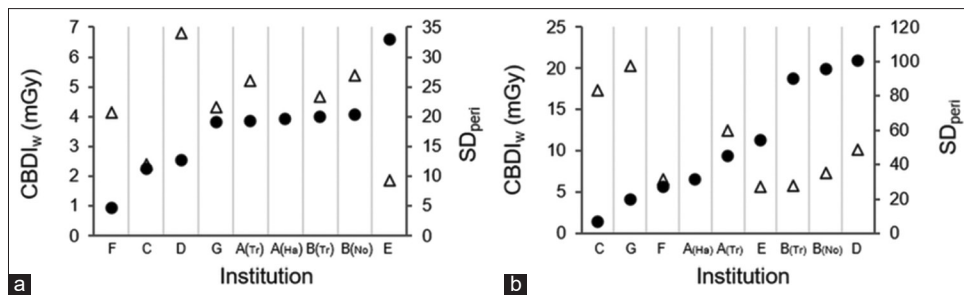
Figure 3: Weighted cone-beam dose index (CBDI_w) (●) and SD_peri (SD value calculated from ROI in peripheral positions only [△]) values of the different institutions, presented in ascending order (from left to right) of CBDI_w values: (a) head protocol; (b) pelvic protocol. Scanning machine initials are in parentheses. CBDI_w: Weighted cone-beam dose index, SD: Standard deviation, ROIs: Regions of interest

phantoms, such as Catphan and water-equivalent phantoms, are generally used.[22,30-33] However, measurement values are strongly dependent on phantom size, shape, and materials. It is difficult to compare imaging dose and image quality with past studies or other institutions unless the measurement equipment and methods are identical. PMMA phantoms are cylindrical acrylic phantoms primarily used for CTDI measurements, but their uniformity also allows for noise evaluation.[22] These phantoms are standardized in terms of features such as phantom size, shape, and materials and are widely used worldwide.[33] PMMA phantoms and pencil chambers are ubiquitous and can be used to evaluate dose and image noise simultaneously and easily. Applying this method may enable multi-institutional surveys to be performed in a simple and unified manner to establish DRLs for radiotherapy.

We observed large dose differences among institutions. Institutions with low imaging doses (institution A, C, F, and G) employed methods for reducing the pelvic imaging dose, while institutions with high imaging doses (institution B, D, and E) used the default mAs value. Such differences in institutional policy lead to significant dose disparities; the maximum difference in imaging dose for the pelvis was 14-fold. Some institutions, such as institution C, employ extreme methods to reduce radiation doses, and it is evident that there is a significant disparity in radiation exposure even when imaging the same body part. Although we examined a limited number of institutions in this study, if we were to investigate a larger number of institutions, we might have obtained even more varied results because of differences in equipment and dose-reduction methods. For image noise, SD_peri ranged from 9.3–34.0 HU and 26.9–97.4 HU for the head and pelvic protocols, respectively, with a maximum difference among institutions of more than 3-fold for both protocols. All institutions used their standard settings, such that it means they can all perform image registration despite significant differences in noise levels. Similarly, Takei *et al*. reported that image registration via manual soft-tissue matching can be performed to within 2 mm despite a low mAs value and high levels of noise.[34] Furthermore, Khan *et al*. created protocols optimized on the basis of studies of scan settings and compared their imaging dose and quality with those of the current default protocol. They reported that

the new protocol allowed for significant dose reduction at most sites without affecting the radiographers' confidence in image registration.[28] These results suggest that further dose reduction, even at a low mAs value, could be achieved in many institutions without compromising the accuracy of imaging registration. Some studies have proposed determining the optimal scan conditions on the basis of image quality, such as the noise level of the bladder (set at 25 HU) and the contrast-to-noise ratio between tissues and background, to optimize IGRT doses.[24,35] However, because of differences in machine characteristics between manufacturers and differences in software versions even with the same machine, the same exposure parameters can result in disparities in dose and image quality.[15,36,37] It is important to understand the characteristics of the machines in one's own institution and identify optimal scan conditions, which depend on many factors in addition to image quality, such as machine type, institutional policies, the use of markers, and operator; this makes it difficult to establish standards for the imaging dose and image quality.[38] Therefore, DRLs, which help us understand the doses in a given facility relative to other facilities, are necessary for radiotherapy. We propose an "image registration reference level" to optimize the IGRT imaging dose. This is especially important given the increasing use of precision radiotherapy, including IGRT.

CONCLUSIONS

In this study, we reported a simple and unified method to access the imaging dose and image quality for IGRT with nine different kV CBCT systems from seven institutions. Our results show that the high imaging dose institutions exhibited approximately 20 mGy to the pelvic phantom, resulting in a 14-fold difference in imaging dose compared to the other institutions. These results suggest the need to establish the DRLs for IGRT imaging dose to guide clinical decision-making.

Conflicts of interest

There are no conflicts of interest.

REFERENCES

1. UNSCEAR 2020/2021 REPORT Vol. I. Scientific Annex A. Sources, Effects and Risks of Ionizing Radiation.
2. UNSCEAR 2008 REPORT Volume I: SOURCES Report to the General Assembly Scientific Annexes A and B. Sources and Effects of Ionization Radiation.
3. ICRP. Recommendations of the ICRP. ICRP Publication 26. Ann ICRP 1977;1:1-53.
4. Vañó E, Miller DL, Martin CJ, Rehani MM, Kang K, Rosenstein M, *et al.* ICRP publication 135: Diagnostic reference levels in medical imaging. Ann ICRP 2017;46:1-144.
5. Murphy MJ, Balter J, Balter S, BenComo JA Jr., Das IJ, Jiang SB, *et al.* The management of imaging dose during image-guided radiotherapy: Report of the AAPM task group 75. Med Phys 2007;34:4041-63.
6. Jaffray DA, Siewerdsen JH. Cone-beam computed tomography with a flat-panel imager: Initial performance characterization. Med Phys 2000;27:1311-23.
7. Létourneau D, Wong JW, Oldham M, Gulam M, Watt L, Jaffray DA, *et al.* Cone-beam-CT guided radiation therapy: Technical implementation. Radiother Oncol 2005;75:279-86.
8. Oldham M, Létourneau D, Watt L, Hugo G, Yan D, Lockman D, *et al.* Cone-beam-CT guided radiation therapy: A model for on-line application. Radiother Oncol 2005;75:271-8.
9. Watt TC, Inskip PD, Stratton K, Smith SA, Kry SF, Sigurdson AJ, *et al.* Radiation-related risk of basal cell carcinoma: A report from the childhood cancer survivor study. J Natl Cancer Inst 2012;104:1240-50.
10. Perks JR, Lehmann J, Chen AM, Yang CC, Stern RL, Purdy JA. Comparison of peripheral dose from image-guided radiation therapy (IGRT) using kV cone beam CT to intensity-modulated radiation therapy (IMRT). Radiother Oncol 2008;89:304-10.
11. Ding A, Gu J, Trofimov AV, Xu XG. Monte Carlo calculation of imaging doses from diagnostic multidetector CT and kilovoltage cone-beam CT as part of prostate cancer treatment plans. Med Phys 2010;37:6199-204.
12. Walter C, Boda-Heggemann J, Wertz H, Loeb I, Rahn A, Lohr F, *et al.* Phantom and *in-vivo* measurements of dose exposure by image-guided radiotherapy (IGRT): MV portal images versus kV portal images versus cone-beam CT. Radiother Oncol 2007;85:418-23.
13. Hyer DE, Hintenlang DE. Estimation of organ doses from kilovoltage cone-beam CT imaging used during radiotherapy patient position verification. Med Phys 2010;37:4620-6.
14. Sykes JR, Amer A, Czajka J, Moore CJ. A feasibility study for image guided radiotherapy using low dose, high speed, cone beam X-ray volumetric imaging. Radiother Oncol 2005;77:45-52.
15. Alaei P, Spezi E. Imaging dose from cone beam computed tomography in radiation therapy. Phys Med 2015;31:647-58.
16. Tegtmeier RC, Ferris WS, Bayouth JE, Miller JR, Culberson WS. Characterization of imaging performance of a novel helical kVCT for use in image-guided and adaptive radiotherapy. J Appl Clin Med Phys 2022;23:e13648.
17. Osei EK, Schaly B, Fleck A, Charland P, Barnett R. Dose assessment from an online kilovoltage imaging system in radiation therapy. J Radiol Prot 2009;29:37-50.
18. Amer A, Marchant T, Sykes J, Czajka J, Moore C. Imaging doses from the Elekta synergy X-ray cone beam CT system. Br J Radiol 2007;80:476-82.
19. Mao W, Gardner SJ, Snyder KC, Wen NW, Zhong H, Li H, *et al.* On the improvement of CBCT image quality for soft tissue-based SRS localization. J Appl Clin Med Phys 2018;19:177-84.
20. Kouno T, Araki F, Nakaguchi Y, Oono T. Dose distribution from kV-cone beam computed tomography in image-guided radiotherapy. Nihon Hoshasen Gijutsu Gakkai Zasshi 2013;69:753-60.
21. Leon SM, Kobistek RJ, Olguin EA, Zhang Z, Barreto IL, Schwarz BC. The helically-acquired CTDI (vol) as an alternative to traditional methodology. J Appl Clin Med Phys 2020;21:263-71.
22. Samei E, Bakalyar D, Boedeker KL, Brady S, Fan J, Leng S, *et al.* Performance evaluation of computed tomography systems: Summary of AAPM Task Group 233. Med Phys 2019;46:e735-56.
23. Wood TJ, Moore CS, Horsfield CJ, Saunderson JR, Beavis AW. Accounting for patient size in the optimization of dose and image quality of pelvis cone beam CT protocols on the Varian OBI system. Br J Radiol 2015;88:20150364.
24. Yang CC, Yu PC, Ruan JM, Chen YC. Optimizing the target detectability of cone beam CT performed in image-guided radiation therapy for patients of different body sizes. J Appl Clin Med Phys 2018;19:310-7.
25. International Atomic Energy Agency, Status of Computed Tomography Dosimetry for Wide Cone Beam Scanners, IAEA Human Health Reports No. 5, IAEA; 2011.
26. Dixon RL, Anderson J, Bakalyar DM, Boedeker K, Boone JM, Cody DD, *et al.* Comprehensive methodology for the evaluation of radiation dose in X-ray computed tomography. Report AAPM Task Group 2010;111:20740-3846.
27. Buckley JG, Wilkinson D, Malaroda A, Metcalfe P. Investigation of the radiation dose from cone-beam CT for image-guided radiotherapy: A comparison of methodologies. J Appl Clin Med Phys 2018;19:174-83.
28. Khan M, Sandhu N, Naeem M, Ealden R, Pearson M, Ali A, *et al.* Implementation of a comprehensive set of optimised CBCT protocols and validation through imaging quality and dose audit. Br J Radiol 2022;95:20220070.
29. International Electrotechnical Commission. Medical Electrical Equipment – Part 2-44: Particular Requirements for the Basic Safety and Essential Performance of X-ray Equipment for Computed Tomography; 2009.
30. Roa AM, Andersen HK, Martinsen AC. CT image quality over time: Comparison of image quality for six different CT scanners over a six-year period. J Appl Clin Med Phys 2015;16:4972.
31. Kuttner S, Bujila R, Kortesniemi M, Andersson H, Kull L, Østerås BH, *et al.* A proposed protocol for acceptance and constancy control of computed tomography systems: A Nordic Association for Clinical Physics (NACP) work group report. Acta Radiol 2013;54:188-98.
32. Colli V, Mangini M, Strocchi S, Lumia D, Canì A, Boffano C, *et al.* Performance assessment of four 64-slice computed tomographic devices for a typical clinical protocol. J Comput Assist Tomogr 2011;35:57-64.
33. International Commission on Radiation Units and Measurements. Phantoms and computational Models in Therapy, Diagnosis and Protection. ICRU Report No. 48; 1992.
34. Takei Y, Monzen H, Matsumoto K, Hanaoka K, Tamura M, Nishimura Y. Registration accuracy with the low dose kilovoltage cone-beam CT: A phantom study. BJR Open 2019;1:20190028.
35. Ordóñez-Sanz C, Cowen M, Shiravand N, MacDougall ND. CBCT imaging: A simple approach for optimising and evaluating concomitant imaging doses, based on patient-specific attenuation, during radiotherapy pelvis treatment. Br J Radiol 2021;94:20210068.
36. Cheng HC, Wu VW, Liu ES, Kwong DL. Evaluation of radiation dose and image quality for the Varian cone beam computed tomography system. Int J Radiat Oncol Biol Phys 2011;80:291-300.
37. Ueltzhöffer S, Zygmanski P, Hesser J, Högele W, Wong J, Bellon JR, *et al.* Clinical application of Varian OBI CBCT system and dose reduction techniques in breast cancer patients setup. Med Phys 2010;37:2985-98.
38. Takei Y, Monzen H, Tamura M, Doi H, Nishimura Y. Dose reduction potential of using gold fiducial markers for kilovoltage image-guided radiotherapy. J Appl Clin Med Phys 2020;21:151-7.